Journal of Innovative Optical Health Sciences
Vol. 6, No. 2 (2013) 1350013 (12 pages)

DOI: 10.1142/S1793545813500132

World Scientific
www.worldscientific.com

IMAGE-BASED *IN VIVO* QUANTITATIVE ASSESSMENT OF HUMAN AIRWAY OPENING AND CONTRACTILITY BY FIBER OPTICAL NASOPHARYNGOSCOPY IN HEALTHY AND ASTHMATIC SUBJECTS

LINHONG DENG*,†,‡
*Institute of Biomedical Engineering and Health Sciences
Changzhou University, Changzhou, Jiangsu 213164, P. R. China
†MOE Key Laboratory of Biorheological Science and Technology
Chongqing University, Chongqing 400044, P. R. China
‡dlh@cczu.edu.cn; denglh@cqu.edu.cn

Received 24 November 2012
Accepted 23 January 2013
Published 20 March 2013

Assessment of human airway lumen opening is important in diagnosing and understanding the mechanisms of airway dysfunctions such as the excessive airway narrowing in asthma and chronic obstructive pulmonary disease (COPD). Although there are indirect methods to evaluate the airway calibre, direct *in vivo* measurement of the airway calibre has not been commonly available. With recent advent of the flexible fiber optical nasopharyngoscope with video recording it has become possible to directly visualize the passages of upper and lower airways. However, quantitative analysis of the recorded video images has been technically challenging. Here, we describe an automatic image processing and analysis method that allows for batch analysis of the images recorded during the endoscopic procedure, thus facilitates image-based quantification of the airway opening. Video images of the airway lumen of volunteer subject were acquired using a fiber optical nasopharyngoscope, and subsequently processed using Gaussian smoothing filter, threshold segmentation, differentiation, and Canny image edge detection, respectively. Thus the area of the open airway lumen was identified and computed using a predetermined converter of the image scale to true dimension of the imaged object. With this method we measured the opening/narrowing of the glottis during tidal breathing with or without making "Hee" sound or cough. We also used this method to measure the opening/narrowing of the primary bronchus of either healthy or asthmatic subjects in response to histamine and/or albuterol treatment, which also provided an indicator of the airway contractility. Our results demonstrate that the image-based method accurately quantified the area change waveform of either the glottis or the bronchus as observed by using the optical nasopharygoscope. Importantly, the opening/narrowing of the airway lumen generally correlated with the airflow and resistance of the airways, and could differentiate the level of airway contractility between the healthy and asthmatic

subjects. Thus, this quantitative assessment of airway opening may provide a useful tool to assist clinical diagnosis of airway dysfunctions and understanding the mechanisms of associated pathophysiologies.

Keywords: Optical nasopharyngoscopy; image processing; glottal aperture; bronchus opening; airway contractility; asthma.

1. Introduction

Bronchial airways in the lungs of a human body constantly open and narrow due to the action of various respiratory muscles as the person breaths. To maintain health, it is critically important to keep the airways' lumen open so that air can be transported through the conducting airways to the alveolar sacks where oxygen exchange takes place. However, in airway disease such as asthma, the airways can narrow excessively when being irritated by certain irritants such as allergen, and thus restrict the airflow through the airways and eventually cause breathing difficulty.[1] In fact, asthma is characterized by bronchial airways that narrow too much and too easily in response to exposure of a variety of contractile stimuli such as histamine. This is often known as airway hyperresponsiveness (AHR).[2] The bronchial airways in asthmatic patients are also known to dilate more than those in nonasthmatic subjects when exposed to bronchodilator, reflecting enhanced level of tone in the airways in asthma. Although the opening/narrowing of the airways is the ultimate determinant of lung function, it has been difficult to directly assess for pulmonary lung function test. Instead, it is usually measured by indirect methods such as spirometry[3] and forced oscillatory technique (FOT).[4]

These indirect methods often provide valuable information regarding the overall state of opening/narrowing of all airways, but not the precise calibre of a given individual airway. These methods have other limitations as well. For example, spirometry, the current standard test for pulmonary airflow, requires active cooperation of the subject, which can be a difficult, impractical or even unfeasible task among certain group of patients such as young children, elderly, paralyzed and unconscious individuals. For these patients, FOT has become the choice of method to assess lung function.[4–7] But the measurement of FOT, i.e., the respiratory impedance could be affected by the motion of non-respiratory structures such as glottis.[8,9] During quiet breathing, the aperture of the laryngeal glottis widens on inspiration and narrows on expiration. During episodic swallowing and speaking, the glottis may also narrow or close abruptly.[10,11] Thus the portion of impedance due to glottis aperture is estimated to range from 20−45% of the total impedance measured by FOT. This represents a significant level of uncertainty associated with the method.[7,12,13]

To overcome the abovementioned limitations, direct and quantitative evaluation of the airway opening/narrowing is desired. With recent advance in flexible optical fiber nasopharyngoscope it has become possible to directly visualize the airway lumen and thus observe the *in vivo* opening/narrowing of the airways.[14] Nevertheless, it has been technically challenging to obtain quantitative assessment of the dynamic process of airway opening/narrowing due to lack of appropriate approach to quantitatively analyze the video images recorded by the nasopharyngoscope. Here, we describe an automatic image processing method that allows for batch analysis of the images recorded during the endoscopic procedure, thus facilitates image-based quantification of the airway opening. We used this method to measure the area changes of both glottis aperture and bronchus lumen for either healthy or asthmatic subjects during different breathing conditions and bronchial treatments. The results demonstrate that the image-based method could not only accurately measure the area of individual airway's open lumen, but also detect abrupt changes of the glottis aperture during respiratory manoeuvre such as coughing and sound-making, or bronchus opening/narrowing in response to bronchoconstrictor/dilator exposure. Importantly, such quantitative assessment could differentiate the opening/narrowing behaviors of the bronchial airways between healthy and asthmatic subjects. These suggest that this image-based method for quantification of airway opening may provide a useful tool to assist clinical diagnosis of airway dysfunction and understanding the mechanisms of associated pathologies.

2. Methods and Materials

2.1. *Volunteer test subjects*

Twenty volunteers including both male and female individuals were recruited as human test subjects in this study. Among them, 10 were healthy individuals, and 10 were clinically diagnosed with moderate asthma, respectively. The age of these volunteers ranged between 16 and 70 years. In addition, none of them had history of smoking, or associated with recent respiratory tract infection. The demographics of the volunteer subjects are presented in Table 1. All protocols used in this study including proper informed consent of subject had been approved by the Institutional Review Board of Human Test Ethics of Chongqing University of Medical Sciences, China. All procedures of nasopharyngoscopy for the purpose of this study were performed by the same physician in the ENT department of the out-patient clinic of No. 1 Hospital of Chongqing, China.

Table 1. Demographics of the volunteer test subjects.

Group	Healthy	Asthmatic
Gender (Male/Female)	6/4	4/6
Age (yr)	34.34 ± 12.81	35.52 ± 13.86
Height (cm)	163.71 ± 7.98	155.86 ± 6.27
Weight (kg)	61.62 ± 8.52	64.52 ± 18.27

2.2. *Visualization of the airway opening/narrowing by nasopharyngoscopy*

In order to observe the airway opening/narrowing, a nasopharyngoscope (Olympus Exera CLV-180, Tokyo, Japan) was used to visualize the cross section of selected part of the airway such as the glottis or bronchus as shown in Fig. 1. The tip of the scope was fitted with a charge coupled device (CCD) camera working in red-green-blue (RGB) color system. The CCD camera continuously takes images inside the airways and then sends the digital signals of the image to be both displayed in real time on the monitor and stored in the memory device of a computer.

2.3. *Calibration of the nasopharyngoscopic scale*

Prior to *in vivo* measurement, the nasopharyngoscope was calibrated to determine the true dimension of the image taken by the CCD camera fitted on the tip of the scope. The calibration was carried out as follows. First, a metric ruler was placed on the top of a table. Then, the CCD camera at the tip of the nasopharyngoscope was placed vertically above the ruler and took image of the ruler at a given height. Subsequently, the CCD camera took images of the ruler at several different heights above the ruler. For each height (distance between the

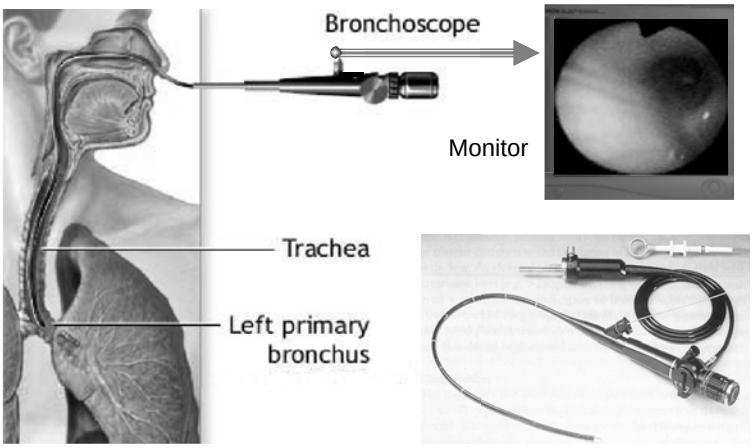

Fig. 1. Illustration of the method to visualize the airway opening/narrowing by flexible fiber optical nasopharyngoscopy. A flexible fiber optical nasopharyngoscope is shown in the lower right panel. The tip of the optical fiber, fitted with a CCD camera was inserted into the airway passage of the test subject through the nasal cavity, and carefully placed near the location of the airway as shown in the left panel. Subsequently, the cross section of the airway lumen was imaged by the CCD camera on the tip of the scope, and the digital image was viewed in real time on the monitor as shown in the upper right panel, as well as stored in the memory device of a computer (not shown).

CCD camera and the ruler, d) at which the ruler was imaged, the number of pixels in the image corresponding to the length of 1 cm on the ruler was counted. Thus, a relationship between d, the distance between the CCD camera and the ruler, and the number of pixels equivalent to 1 cm length was established.

With this relationship, an object of unknown size can be measured for its dimension by imaging the object with the CCD camera at a given distance, d, from the object and then converting the pixels of the object's image to dimension in length unit (cm). During nasopharyngoscopy, however, the actual distance between the CCD on the scope tip and the airway cross section could not be determined directly. To solve this problem, the scope tip was inserted into the airway passage at different depths and thus took images of the same airway cross section at two or more different distances and the relative distances between images taken were recorded. Using the relative distances, the true dimension of the imaged airway cross section could be obtained by solving the two-variable function of the above-mentioned relationship between d and the number of pixels.

2.4. *Experimental protocols*

Before the procedure of nasopharyngoscopy, the subject was given a thorough explanation of what was to be done, the indications for the procedure, and any alternatives, if they existed.[14,15] The subject was then placed in a medical examination chair in slightly reclined sitting position for comfort. In order to prevent irritation and discomfort caused by the insertion of the nasopharyngoscope into the airway passage, the subject was given a puff of topical anesthetic (xylocaine spray 10%) to the nostrils. Additional topical nasal decongestant, Otrivin (Novartis Inc., Hong Kong, China) might also be administered to the nostril if the nasal passage of the subject was congested. Once the effect of anesthesia was confirmed, the scope was carefully inserted through the airway passage, while being kept away from the airway wall, until the target location of the airway was in view.

The scope was kept steady in the position and observed the airway lumen until the breathing pattern had stabilized and the respiratory movements of the airway appeared to be reproducible. Subsequently, the images of the airway taken by the CCD camera were continuously recorded and stored on computer. In this study, two protocols were employed. The first protocol was carried out to examine the glottis opening/narrowing during either normal breathing or normal breathing with a single cough and 5 s "Hee" sound. During the procedure of nasopharyngoscopy, the scope was inserted near and focused on the glottis, and then continuously recorded images of the glottis for 1 min while the subject breathed normally, followed by another 1 min during which the subject was asked to either perform 5 s of "Hee" sound or act a single cough at the given time points.

The second protocol was carried out to examine the opening/narrowing of the bronchus either during normal breathing or in response to stimulation for bronchial constriction and dilation. During this experiment, the scope was inserted near and focused on the opening of the left primary bronchus, and then continuously recorded images of the bronchus for one minute during normal breathing. Subsequently, the subject was asked to breath tidally through the nebulizer mouthpiece with which normal saline was administered for 30 s. After another 30 s, the subject breathed in nebulized histamine solutions for 30 s with successively increasing concentration from 0.3 to 8 mg/ml, at 90 s intervals. After another 30 min, nebulized albuterol at 2.5 mg/ml was delivered through the nebulizer mouthpiece to the subject for 30 s while the bronchus was imaged and recorded continuously for another 30 min.

2.5. *Image processing and analysis*

The original RGB images recorded were batch processed to convert them into grayscale format. Then, each of the grayscale images was further processed by using a custom developed image processing method that combined several techniques including Gaussian smoothing filter, threshold segmentation, differentiation, and Canny image edge detection. This method allowed fast and effective detection of the moving edge of the airway lumen, a task not possible to accomplish by conventional image-based edge detection method.[16–18] The algorithm software was developed on Matlab® computing platform (The MathWorks Inc., Nortic, MA, USA) and executed by a computer with an Intel Pentium 4 processor at 2.8 GHz. The key components of the algorithm were further described in the following.

Image smoothing is a technique that averages the image data points with their neighbors in the image. The primary reason for smoothing is to increase the signal to noise ratio, therefore smoothing is often referred as filtering because it has the effect of suppressing high frequency signal and enhancing low frequency signal. In particular for this study, the Gaussian smoothing filter was employed to smooth the images. The Gaussian filter was a linear convolution filter based on a filter kernel that was convoluted with an image. The Gaussian width was specified either with qualifier sigma or as a default value of 1.5 pixels. The filter kernel itself was considered and viewed as either a curve in one dimension (1D) or an image in two dimensions (2D).

For 1D and 2D image, the mathematic formula of the Gaussian filter was derived as follows, respectively.

$$K_{1D} = e^{\frac{-i2}{2 \cdot SD2}}, \tag{1}$$

$$K_{2D} = e^{\frac{-i2}{2 \cdot SDx2}} e^{\frac{-j2}{2 \cdot SDy2}}, \tag{2}$$

where SDx and SDy are the standard deviations for the x- and y-direction, respectively.

Once being smoothed, the image was processed by the fixed threshold segmentation technique. This technique used fixed threshold to divide pixels within the image into two areas. Those pixels whose intensity values were greater than the threshold were kept unchanged, but those whose intensity values were less than the threshold were reset so that their intensity values all became zero. Depending on the brightness of the recorded image, a threshold of 20 to 30 could separate the pixels in the area of the airway lumen that often appeared almost pitch black from those outside the lumen. After the segmentation, the area of airway lumen was turned into a uniformly black area. Subsequently, the image was mathematically differentiated along each row of the pixels to determine the points at which the pixels exhibited greatest change in intensity, and usually represented the boundary of the airway lumen.

In order to identify a continuous and clearly-cut edge of the open airway lumen, the image was further analyzed by the Canny edge detection.[18] Canny edge detection applied both a low and a high threshold to the intensity gradient of pixels in the image. If the intensity gradient of a pixel was above the high threshold, there was a clear edge at that point and the pixel was therefore described as an edge pixel. Otherwise, if the intensity gradient of the pixel was below the low threshold, there appeared no clear edge around this point and thus the pixel was described as a nonedge pixel. The pixel with intensity gradient in between could be an edge pixel if it was connected to a definite edge pixel either directly or via other pixel whose intensity gradient was between the low and high thresholds.[18,19] These edge pixels finally identified the area of the open airway lumen.

2.6. *Statistical analysis*

All values were expressed as mean±standard deviation (SD). Statistic analysis for multiple comparisons were performed with one-way analysis of variance (ANOVA) followed by Tukey test using SigmaPlot 12.0 (SysStat Software, San Jose, CA). A level of $p < 0.05$ was accepted as statistically significant.

3. Results

Figure 2 shows that calibration of the nasopharyngoscope resulted in a nonlinear relationship between Y and d, where Y was the conversion factor, or number of pixels in the image corresponding

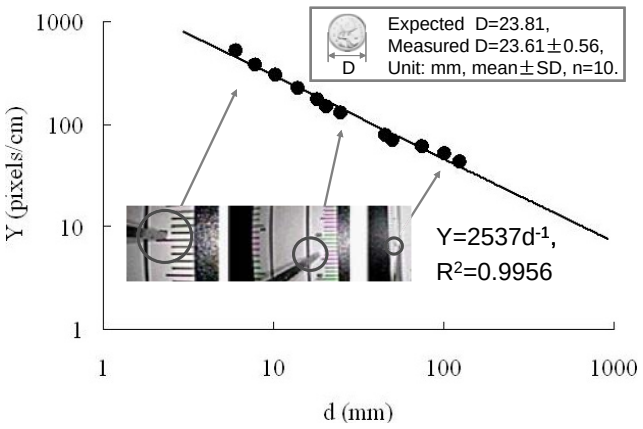

Fig. 2. The relationship between the conversion factor (Y) and the distance (d) of the CCD camera on the scope tip from the object to be imaged. The conversion factor Y was defined as the ratio of the image size or number of pixels to its actual metric size of an object that was imaged. The image size varied depending on the distance from which the object was imaged as demonstrated by the images in the lower insert. In the case of the nasopharyngoscope used in this study, Y decreased with increasing d as a power-law function, represented by the solid line that closely fitted the measurement data.

to 1 cm length of the object, and d was the distance between the CCD camera on the scope tip and the object imaged. In this case, the object was the metric scale on a ruler. This relationship could be closely fitted by a power-law function, $Y = 2537\,\mathrm{d}^{-1}$, shown as solid line in Fig. 2 ($R^2 = 0.9956$). The accuracy of this calibration function was verified by imaging a coin of which the diameter was known ($D = 24.02$ mm). The coin was imaged by the nasopharyngoscope while the tip of the scope was held at different distances from the coin. From each image of the coin, the diameter of the coin was calculated by the number of pixels corresponding to the centerline of the imaged coin and the conversion factor for the distance (d). The mean diameter of the coin as measured by this image-based method turned out to be 23.68 mm, which was within an accuracy of 98.59%.

Figure 3 demonstrates an example of using the image-based method to visualize and quantify the area of glottis opening for one subject. Figures 3(a) to 3(d) display the grayscale image that was converted from the original RGB image of the subject's glottis captured by the scope's CCD camera, and the images resulted from Gaussian smooth filtering, segmentation, and Canny edge detection of the grayscale image, respectively. The white line superimposed on the glottis image in Fig. 3(d) indicated the borderline of the glottis opening and the area within this borderline was computed as the area of glottis opening (A_g, cm^2).

By analyzing the images captured continuously by the scope in time sequence, the opening/narrowing of the glottis could be quantitatively measured and tracked with time. Therefore, the image-based method was not only able to produce highly accurate measurement of the opening area of the airway structure, but also closely follow the opening and narrowing of the airway structure such as the glottis aperture. Indeed, the results of time sequential analysis revealed that the area of the glottis opening fluctuated with time even during quiet breathing as shown in Fig. 3(e). The respiratory resistance measured simultaneously by forced oscillatory technique also exhibited periodic fluctuation in similar pattern during quiet breathing. However, the time course of the measured glottis opening area clearly shows that the aperture of the laryngeal glottis opened on inspiration and narrowed on expiration (Figs. 3(e) versus 3(f)). The widening generally commenced before the onset of

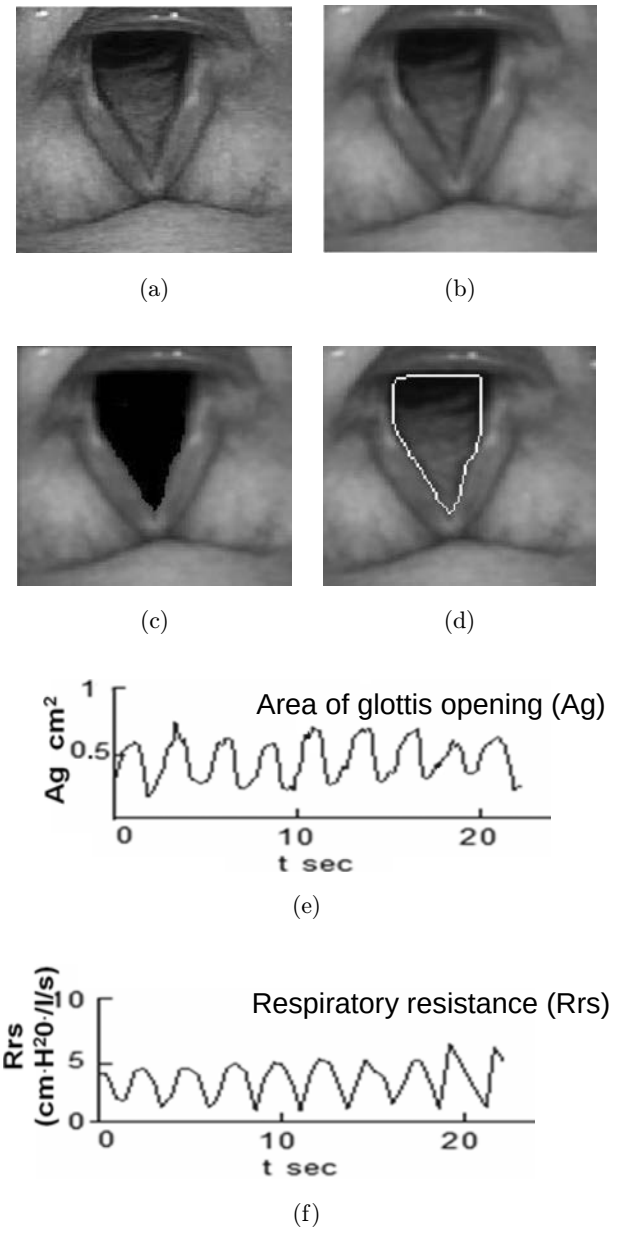

Fig. 3. Area of glottis opening and its fluctuation with time as measured by the image-based method. (a) Grayscale image of the glottis, which was obtained by converting the original RDB image captured by the CCD camera of the nasopharyngoscope. (b)−(d) Images resulted from Gaussian smooth filtering, pixel segmentation, and Canny edge detection, respectively, of the grayscale image of the glottis. These image processing algorithms together identified the edge of the glottis aperture (outlined by the white line in (d)), from which the area of glottis opening (A_g) was computed. (e),(f) The time course of fluctuation of glottis opening (A_g), and the respiratory resistance (R_{rs}), respectively.

inspiration, whereas the narrowing preceded the onset of expiration, respectively.

The upper panel of Fig. 4 shows representative images of the glottis during normal breathing,

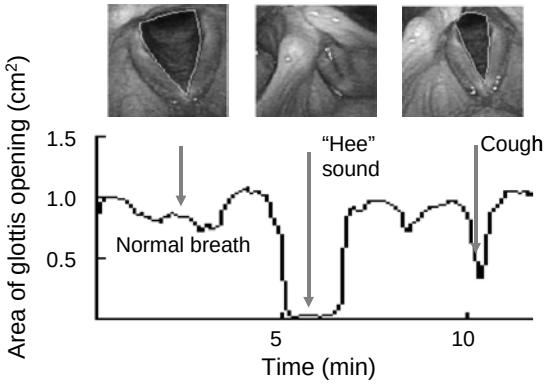

Fig. 4. Opening and narrowing of the glottis aperture with different breathing maneuvers. Upper panel from left to right: representative image of the glottis during either normal breathing, "Hee"-sound making, or coughing, respectively. The edge of the opening glottis aperture was marked by the white line. Lower panel: Time course of the area of glottis opening quantified by the image-based method during the same breathing maneuvers.

"Hee"-sound making, or coughing, respectively. The left image shows that the glottis aperture remained fairly open during normal breathing. When the subject was asked to make a "Hee" sound for about 5 s or to act a single cough, the glottis aperture immediately narrowed, and then quickly re-opened to the state as in normal breathing. During the period of making "Hee" sound, the subject's glottis kept almost completely closed up (the middle image). The single cough, however, induced more than half way down narrowing, but not complete closure of the glottis (the right image). Accordingly, the lower panel of Fig. 4 shows the change wave of the area of glottis opening (A_g) of the subject, as quantitatively assessed by the image processing method. It can be seen that A_g fluctuated to a certain extent during normal breathing. The crest and the trough of the wave corresponded to the inspiration and expiration, respectively. When the subject made a 'Hee' sound, the area of glottis opening (A_g) was reduced to almost zero, reflecting a state of nearly complete closure of the glottis for a few seconds. In contrast, when the subject made a single cough, the glottis area, A_g was reduced to a large extent but not near zero, reflecting a great deal of narrowing but no closure of the glottis due to cough. In addition, the narrowing of the glottis due to cough lasted only momentarily and then the glottis quickly reopened to the level of opening during normal breathing, which corresponded to the transient nature of the single cough.

Similarly as described above, the cross section of the left primary bronchus was also imaged by the flexible fiber optical nasopharyngoscope, and the area of the bronchus open lumen was thus quantitatively assessed using the image processing method. From left to right, Fig. 5 displays representative images of the bronchus of a test subject during normal tidal breathing, 5 min post histamine challenge, and 5 min post albuterol treatment following histamine challenge, respectively. During normal tidal breathing, the cross sectional area of the bronchus lumen appeared to fluctuate in similar manner as that of the glottis aperture, but on average the airway lumen remained fairly open over time (Fig. 5(a)). In response to challenge of inhaled nebulized histamine, the bronchus began to narrow down. After about 5 min from inhaling histamine the narrowing reached maximum and the area of the bronchus lumen stabilized at a reduced level as compared to that prior to histamine challenge (Fig. 5(b)). In addition to the narrowing of the bronchus lumen, the fluctuation of the cross-sectional area of the bronchus was also reduced after

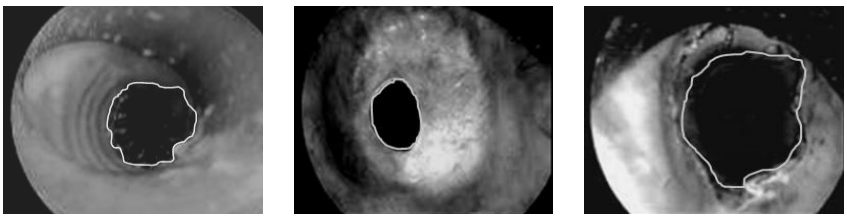

(a) (b) (c)

Fig. 5. Representative images of the primary bronchus with the area of bronchus opening assessed by the image-based method. The bronchus was imaged by the flexible fiber optical nasopharyngoscope, and the area of the bronchus opening was identified (outlined by the while line) and computed by the image processing and analysis algorithm. (a)−(c) displays the area of bronchus opening during normal tidal breathing, 5 min after the last dose of histamine challenge, and 5 min after albuterol treatment (2.5 mg/ml) following 30 min waiting time at the end of the last dose histamine challenge, respectively.

the histamine challenge (data not shown). Subsequent to the histamine challenge, inhalation of nebulized albuterol caused the bronchus to reopen up and completely recover from the contracted state induced by histamine challenge (Fig. 5(c)).

Figure 6 shows the dose response of the bronchus opening to challenge of histamine in increasing concentration for either the normal or asthmatic subjects. As the subject inhaled nebulized histamine, the subject's bronchus generally narrowed, but the extent of narrowing depended on the concentration of histamine solution. For the normal subjects, the area of the left primary bronchus was $0.53 \pm 0.18\,\text{cm}^2$ (mean $\pm$ SD, $n = 10$). When challenged by histamine at concentration below 1 mg/ml, the bronchus appeared to narrow only slightly, but not significantly from that treated with saline solution (Control). As the histamine concentration increased to 3 mg/ml, the bronchus narrowed significantly as compared to Control. The narrowing was further enhanced as the histamine concentration increased to 6 mg/ml, and then stabilized as the histamine concentration increased from 6 mg/ml to 8 mg/ml (gray line in Fig. 6). For the asthmatic subjects as compared to the normal subjects, the calibre of the bronchus appeared to be smaller even in the absence of histamine challenge (0.48 ± 0.24 versus $0.53 \pm 0.18\,\text{cm}^2$, $p < 0.05$, $n = 10$). As challenged by histamine with increasing concentration from 0.3 mg/ml to 8 mg/ml, the bronchus of the asthmatic subjects narrowed down consistently (black line in Fig. 6). More importantly, in the asthmatic group, not only the bronchus calibre was significantly smaller than that of the normal subjects, but also the extent of bronchus narrowing was greater at every dose of histamine challenge. Even at the low dose of histamine concentration below 1 mg/ml, the bronchus of the asthmatic group already exhibited significant narrowing from that prior to histamine challenge, indicating both greater responsiveness and sensitivity of the asthmatic airways to the challenge of histamine.

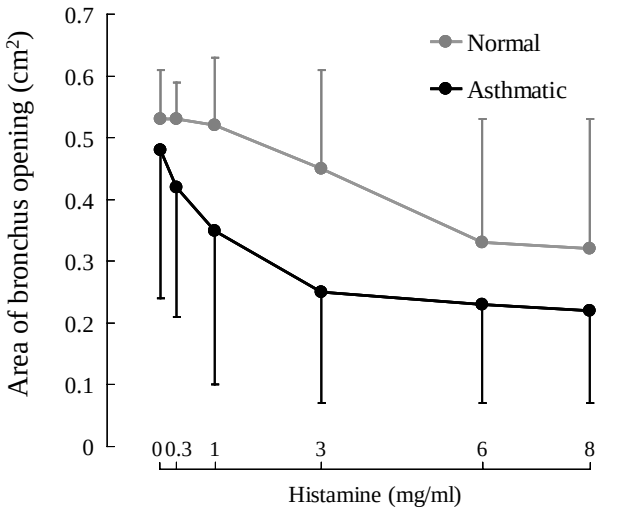

Fig. 6. Area of bronchus opening before and after histamine challenge. The bronchus opening was quantitatively assessed by the image-based method during tidal breathing while inhaling either saline solution without histamine (0 mg/ml), or with histamine at consecutively increasing concentration from 0.3 mg/ml to 8 mg/ml, respectively. The results are given as mean $\pm$ SD. *, # indicates $p < 0.05$ and 0.01, respectively for comparison between normal and asthmatic groups at each dose, $n = 10$.

This greater responsiveness and sensitivity to histamine challenge can be demonstrated alternatively by the percentage (%) of change in area of bronchus opening as shown in Fig. 7. This was defined as $((A_0 - A_i)/A_0)$*100, where A_0, A_i are the areas of bronchus opening prior to histamine challenge and after histamine challenge at a given dose, respectively. In this way, the relative amount of bronchus narrowing after histamine challenge can be equally compared between the normal and asthmatic groups. It can be seen from Fig. 7 that both the normal and asthmatic groups exhibited increasing amount of airway narrowing in response to increasing concentration of histamine. However, the curve of % change of bronchus opening versus histamine concentration for the asthmatic group

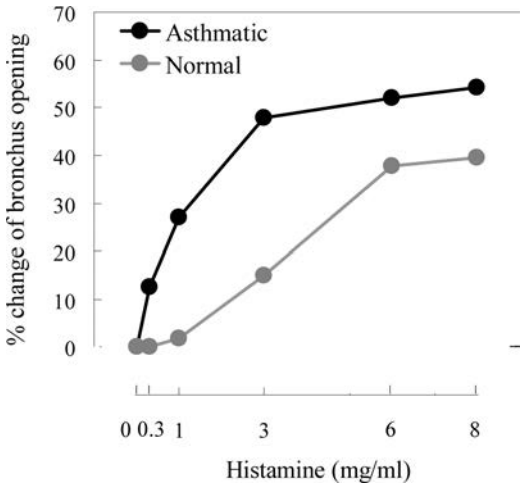

Fig. 7. Percentage of change in area of bronchus opening in response to histamine challenge for the normal and asthmatic groups.

has clearly shifted both upward and leftward from that for the normal group. Such shift in the parallel comparison unequivocally demonstrates the greater responsiveness and sensitivity to histamine challenge in the asthmatic subjects.

Subsequent to the histamine challenge, inhalation of nebulized albuterol (2.5 mg/ml) led to relaxation and thus reopening of the bronchus in both the normal and asthmatic groups. The bronchus relaxation reached maximum when the subject inhaled nebulized albuterol at 2.5 mg/ml for 30 s and the bronchus opening was assessed at 5 min post albuterol inhalation. Figure 8 displays the results of the area of bronchus opening during either tidal breathing, maximally contracted (5 min post-inhalation of histamine at 8 mg/ml), maximally relaxed (5 min post-inhalation of albuterol at 2.5 mg/ml for 30 s), respectively. It can be seen that for both the normal and asthmatic groups the area of bronchus opening recovered from the maximally contracted level after 5 min of inhaling 2.5 m/ml albuterol for 30 s. In some cases, particularly in the asthmatic group, albuterol treatment resulted in greater area of the bronchus opening as compared to that during tidal breathing. Considering that the bronchus of the asthmatic group responded to histamine challenge with greater narrowing, it would be meaningful to compare the contractile scope of the bronchus between the normal and asthmatic groups as shown in the middle of Fig. 8. The contractile scope was defined as the difference in the area of bronchus opening between the maximally relaxed and the maximally contracted states as relative to that during tidal breathing, which reflected the total contractility of the bronchus. Apparently, the bronchus of the asthmatic group exhibited a greater contractile scope as compared to the normal group (72.9% versus 43.4%, respectively).

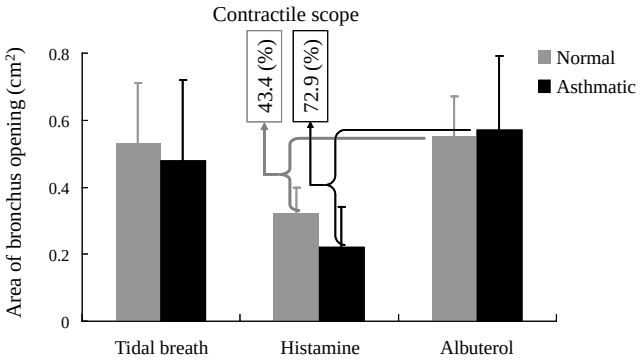

Fig. 8. Comparison of the areas of bronchus opening for either normal or asthmatic subjects in the absence or presence of histamine/albuterol challenge. The results for the normal, asthmatic subjects are presented as gray, black bars, and as mean±SD, respectively. Histamine and Albuterol represent the opening areas of the bronchus that was either maximally contracted (5 min post inhalation of histamine at 8 mg/ml) or maximally relaxed (5 min post inhalation of albuterol at 2.5 mg/ml for 30 s). Contractile scope indicates the difference of bronchus opening between the maximally relaxed (Albuterol) and maximally contracted (Histamine) conditions as percentage of the area of bronchus opening during tidal breathing.

4. Discussion

The primary goal of this study was to develop an image-based method that could quantitatively assess the opening/narrowing of the pulmonary airways by using flexible fiber optical nasopharyngoscopy. In order to do so, we took advantage of various image processing techniques and integrated them into the method as described in this report. This method was capable of analyzing large amount of image data in batch, thus quickly identifying and computing the area of the airway lumen cross section. We used this method to evaluate the opening/narrowing of glottis aperture of normal subjects during different maneuver of breathing, as well as that of the primary bronchus of both the normal and asthmatic subjects in the absence or presence of bronchial challenge. We demonstrated that this method could generate highly reproducible and accurate measurement of the time-varying opening area of the airway structure such as the glottis aperture and the bronchus.

For the glottis aperture, its opening area fluctuated with time even during normal quiet tidal breathing. When the subject exercised active respiratory maneuver such as making "Hee" sound or cough, the glottis aperture abruptly narrowed or even nearly closed. The image-based method not only captured the quick narrowing and opening of the glottis but also accurately quantified the change in the area of the glottis opening. The change wave of the quantified area of glottis opening corresponded well to the glottis fluctuation as observed in the video sequence. For the bronchus, the image-based method also demonstrated a strong capability of identifying and quantifying the area of the bronchus opening. Thus, the fluctuation of the bronchus calibre during normal tidal breathing, and the narrowing or opening of the bronchus in

response to stimulation of either contraction or relaxation was directly and quantitatively assessed. Furthermore, the quantitative assessment of the bronchus opening/narrowing was able to clearly differentiate the bronchus behaviors between the normal subjects and the asthmatic patients.

To our knowledge, there have been few attempts to establish method for quantitative assessment of the video recorded images captured by nasopharyngoscope, especially as a tool to quantitatively assess the respiratory function. In the early 1961, Rattenborg examined the respiratory movement using indirect techniques.[20] Later, Jackson *et al.* observed the movement of glottal aperture during panting.[21] England *et al.*[11] measured glottic width during quiet breathing. Although these studies attempted to assess the opening of airway structure such as glottal aperture and its influence on pulmonary airflow, they were neither direct nor quantitative. And the indirect and qualitative techniques could hardly be able to obtain accurate measurement of the dimensions of the airway structure, and follow the dynamic process of the airway opening/narrowing.

With the image-based method reported here, the accuracy of measurement of the airway opening depended largely on the determination of the distance between the tip of the scope and the airway structure to be imaged. The well-known error sources included the resolution of the tool to measure distance and reliability of the operator who took the measurement. These errors could be either controlled or well estimated. However, there could be other error sources that were not well understood, and therefore hard to manage or evaluate. One particular factor to be considered was the angle between the scope and the imaged target such as the glottis.[10] For example, when imaging the glottis, the scope tip was assumed to be held in right angle (90°) or vertical to the cross sectional plane of the glottis, but a small tilt was almost impossible to notice and avoid. It was estimated that the tilt angle between a rigid endoscope and the larynx was less than 10°.[22] The accuracy of such estimate, however, could be questioned because the angle was difficult to directly visualize. Nevertheless, there have been efforts to correct the tilt effect on the image measurement by using numerical method and correction algorithms.[23–25] Each of these corrections was developed only for a specific type and design of the scope in use, and not universally applicable. Further solution for the tilt effect would depend on new design of the scope, allowing easy and precise determination of the distance between the scope tip and the imaged airway structure. Therefore, we only assumed in this study that the scope tip was held in 90° vertically to the imaged airway cross section, and thus did not correct the images for the tilt effect. This would no doubt contribute to limit accuracy of our measurements.

Despite the limitations, the results of our measurements turned out to be consistent with those reported in the literature, suggesting that the accuracy of the presented method was acceptable. For example, the average area of the glottis aperture as measured by our image-based method with 10 healthy human subjects was $0.98\,\mathrm{cm}^2$. This estimation was in good agreement with that from computational calculation by Rigau *et al.*[13] In addition, the change wave of the quantified area of glottis aperture opening as obtained by our image-based assessment clearly revealed that the glottis aperture opened on inspiration and narrowed on expiration during quiet breathing, which was in agreement with previous visual observations reported by Baier *et al.*[26] and Brancatisano *et al.*[27] It should be noted that while the measurement was highly reproducible for a given individual, the variations between individual subjects were considerably large (∼30%). These large variations could be in part due to the small sample size ($n = 10$) used in this study, or the inherent difference in the airway anatomies between the individuals.

When the bronchus was assessed by the image-based method, the results not only show the narrowing and reopening of the bronchus in response to contractile, and relaxant agonist, in this case histamine, and albuterol, respectively, but also clearly differentiated the airway behaviors between the normal and the asthmatic subjects. The dose and time dependence of the bronchus opening on histamine challenge was generally consistent with other reports from both *in vivo* and *in vitro* studies. More importantly, this image-based method directly demonstrated that the bronchus of the asthmatic subjects narrowed more easily and profoundly when challenged by histamine as compared to their normal counterparts. This feature of airway behavior for the asthmatics is widely known as bronchial airway hyperresponsiveness (AHR), and is one of the hallmarks associated with asthma. The relationship between AHR and the airway narrowing

is often inferred, based on the model of respiratory mechanics, by the measured change of airway resistance in response to stimulation of contraction. Evaluation of AHR by *in vivo* measurement of the area change of the airway lumen, on the other hand, would provide first-hand information regarding the structure and function of the bronchial airways.

Furthermore, it was noted that in response to histamine challenge, not only the bronchus narrowed more but the variability, i.e., the standard deviation of the measured area of bronchus opening also increased as the histamine dose increased for the normal subjects. For the asthmatic subjects, the variability of the bronchus opening was greater than that for the normal subjects even in the absence of histamine challenge. But the level of variability in the asthmatics did not seem to be influenced by the increasing dose of histamine challenge. This observation of greater variability of airway opening for the asthmatic subjects was consistent with that reported by Que *et al.*,[28] and is thought to be a characteristic feature of asthma. For the normal subjects, the increased variability of bronchus opening with increasing dose of histamine implied that the challenged normal bronchus might alter its behavior to be more like asthmatic. Another feature associated with asthma is the greater contractility also known as airway tone, i.e., the asthmatic airways, as compared to the normal ones, can be dilated (opened) to a greater extent in response to relaxant agonist such as albuterol.[29] This feature was also captured by the quantitative assessment of the bronchus opening using the image-based method, as indicated by the different contractile scopes between the normal and the asthmatic subjects. The existence of great contractility or tone in the airway wall of asthmatic airways has been attributed to contribute in the stiffening and remodeling of the airway tissues such as airway smooth muscle,[30] which may play an important role in worsening and exacerbation of asthma. Thus, the airway contractility or tone, as quantitatively assessed in this study, could be a useful indicator for monitoring the procession and severity of asthma.

5. Conclusion

In conclusion, the image-based method presented in this report integrated processing and analysis algorithms to identify and quantitatively assess the airway opening/narrowing. Using this method, not only the area of airway opening and its fluctuation could be accurately measured during normal quiet tidal breathing, but also the quick and transient events of airway opening/narrowing could be monitored and quantitatively evaluated. The results from tests on either the glottis aperture or the bronchus provided a proof of concept for this method to automatically and quantitatively characterize the structure and functional behavior of the airways as imaged by the nasopharyngoscope. If further validated, this method would provide a valuable assistance tool to liberate clinicians from laborious manual examination of the images, and thus help diagnosis and treatment of airway diseases such as vocal cord dysfunction, and asthma.

Acknowledgment

This work is partly supported by grants from Natural Science Foundation of China (Grant No. 11172340), Training Program for Hundreds of Distinguished Leading Scientists of Chongqing, Chongqing Natural Science Foundation (Project No. CSTC, 2010BA5001), and Sharing Fund of Chongqing University Large-Scale Equipment (Nos. 2010063057, 2011063048, and 2011063049).

References

1. C. L. Grainge, L. C. Lau, J. A. Ward *et al.*, "Effect of bronchoconstriction on airway remodeling in asthma," *N. England J. Med.* **364**, 2006−2015 (2011).
2. V. Brusasco, E. Crimi, R. Pellegrino, "Airway hyper-responsiveness in asthma: Not just a matter of airway inflammation," *Thorax* **53**, 992−998 (1998).
3. M. R. Miller, R. Crapo, J. Hankinson *et al.*, "General considerations for lung function testing," *Eur. Respir. J.* **26**, 153−161 (2005).
4. E. Oostveen, D. MacLeod, H. Lorino *et al.*, on behalf of the ERS Task Force on Respiratory Impedance Measurements, "The forced oscillation technique in clinical practice: Methodology, recommendations and future developments," *Eur. Respir. J.* **22**, 1026−1041 (2003).
5. M. D. Goldman, "Clinical application of forced oscillation," *Pulmon Pharmacol. Ther.* **14**, 341−350 (2001).
6. S. Srikasibhandha, "Measurement of respiratory resistance in newborn infants with the oscillation method," *Anaesthesist* **32**, 214−218 (1983).

7. R. Peslin, J. Felicio da Silva, C. Duvivier, F. Chabot, "Respiratory mechanics studied by forced oscillations during artificial ventilation," *Eur. Respir. J.* **6**, 772−784 (1993).
8. E. N. Bruce, "Temporal variations in the pattern of breathing," *J. Appl. Physiol.* **80**, 1079−1087 (1996).
9. N. J. Vincent, R. Knudson, D. E. Leith, P. T. Macklem, J. Mead, "Factors influencing pulmonary resistance," *J. Appl. Physiol.* **29**, 236−243 (1970).
10. S. H. Dailey, J. B. Kobler, R. E. Hillman, K. Tangrom, E. Thananart, M. Mauri, S. M. Zeitels, "Endoscopic measurement of vocal fold movement during adduction and abduction," *Laryngoscope* **115**, 178−183 (2005).
11. S. J. England, D. Bartlett Jr., J. A. Daubenspeck, "Influence of human vocal cord movements on airflow and resistance during eupnea," *J. Appl. Physiol.* **52**, 773−779 (1982).
12. J. Rigau, R. Farre, J. Roca, S. Marco, A. Herms, D. Navajas, "A portable forced oscillation device for respiratory home monitoring," *Eur. Respir. J.* **19**, 146−150 (2002).
13. J. Rigau, R. Farre, X. Trepat, D. Shusterman, D. Navajas, "Oscillometric assessment of airway obstruction in a mechanical model of vocal cord dysfunction," *J. Biomech.* **37**, 37−43 (2004).
14. R. A. Strauss, "Flexible endoscopic nasopharyngoscopy," *Atlas Oral Maxillofac. Surg. Clin. North Am.* **15**, 111−128 (2007).
15. P. Czaja, J. Soja, P. Grzanka, A. Cmiel, A. Szczeklik, K. Sladek, "Assessment of airway caliber in quantitative videobronchoscopy," *Respiration* **74**, 432−438 (2007).
16. C. Chen, J. F. Ma, J. J. Bu, K. Hou, S. L. Bao, "An energy conduction model for cell image segmentation," *Chin. Sci. Bull.* **56**, 1048−1054 (2011).
17. Y. S. Yin, X. Y. Zhao, X. F. Tian, J. Li, "Feature-point-extracting-based automatically mosaic for composite microscopic images," *Chinese Sci. Bull.* **52**, 1291−1295 (2007).
18. J. Canny, "A computational approach to edge-detection," *IEEE Trans. Pattern Anal. Mach. Intell.* **8**, 679−698 (1986).
19. Y. Zhang, E. Bieging, H. Tsui, J. J. Jiang, "Efficient and effective extraction of vocal fold vibratory patterns from high-speed digital imaging," *J. Voice* **24**, 21−29 (2010).
20. C. Rattenborg, "Laryngeal regulation of respiration," *Acta Anaesthesiol. Scand.* **5**, 129−140 (1961).
21. A. C. Jackson, P. J. Gulesian Jr., J. Mead, "Glottal aperture during panting with voluntary limitation of tidal volume," *J. Appl. Physiol.* **39**, 834−836 (1975).
22. D. G. Hanson, J. Jiang, M. D'Agostino, G. Herzon, "Clinical measurement of mucosal wave velocity using simultaneous photoglottography and laryngostroboscopy," *Ann. Otol. Rhinol. Laryngol.* **104**, 340−349 (1995).
23. K. V. Asari, S. Kumar, D. Radhakrishnan, "Technique of distortion correction in endoscopic images using a polynomial expansion," *Med. Biol. Engrg. Comput.* **37**, 8−12 (1999).
24. E. Kouwenhoven, F. Mast, G. L. van Rijk-Zwikker, "Geometrical reconstruction of images obtained with electronic endoscopy," *Phys. Med. Biol.* **38**, 13−24 (1993).
25. W. E. Smith, N. Vakil, S. A. Maislin, "Correction of distortion in endoscope images," *IEEE Trans. Med. Imag.* **11**, 117−122 (1992).
26. H. Baier, A. Wanner, S. Zarzecki, M. A. Sackner, "Relationships among glottis opening, respiratory flow, and upper airway resistance in humans," *J. Appl. Physiol.* **43**, 603−611 (1977).
27. T. Brancatisano, P. W. Collett, L. A. Engel, "Respiratory movements of the vocal cords," *J. Appl. Physiol.* **54**, 1269−1276 (1983).
28. C. L. Que, C. M. Kenyon, R. Olivenstein, P. T. Macklem, G. N. Maksym, "Homeokinesis and short-term variability of human airway calibre," *J. Appl. Physiol.* **91**(3), 1131−1141 (2001).
29. R. A. Panettieri, M. I. Kotlikoff, W. T. Gerthoffer, M. B. Hershenson, P. G. Woodruff, I. P. Hall, S. Banks-Schlegel, "Airway smooth muscle in bronchial tone, inflammation, and remodelling," *Amer. J. Respir. Crit. Care Med.* **177**, 248−252 (2008).
30. L. Deng, N. J. Fairbank, D. J. Cole, J. J. Fredberg, G. N. Maksym, "Airway smooth muscle tone modulates mechanically induced cytoskeletal stiffening and remodelling," *J. Appl. Physiol.* **99**, 634−641 (2005).